Geochemical Perspectives Letters

Formation of Archean continental crust constrained by boron isotopes

M.A. Smit[1*], A. Scherstén[2], T. Næraa[2], R.B. Emo[1,3], E.E. Scherer[4], P. Sprung[5], W. Bleeker[6], K. Mezger[7], A. Maltese[7], Y. Cai[8], E.T. Rasbury[9], M.J. Whitehouse[10]

OPEN ACCESS

doi: 10.7185/geochemlet.1930

Abstract

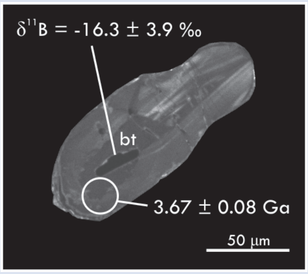

The continental crust grew and matured compositionally during the Palaeo- to Neoarchean through the addition of juvenile tonalite-trondhjemite-granodiorite (TTG) crust. This change has been linked to the start of global plate tectonics, following the general interpretation that TTGs represent ancient analogues of arc magmas. To test this, we analysed B concentrations and isotope compositions in 3.8-2.8 Ga TTGs from different Archean terranes. The $^{11}B/^{10}B$ values and B concentrations of the TTGs, and their correlation with Zr/Hf, indicate differentiation from a common B-poor mafic source that did not undergo addition of B from seawater or seawater-altered rocks. The TTGs thus do not resemble magmatic rocks from active margins, which clearly reflect such B addition to their source. The B- and ^{11}B-poor nature of TTGs indicates that modern style subduction may not have been a dominant process in the formation of juvenile continental crust before 2.8 Ga.

Received 11 June 2019 | Accepted 18 October 2019 | Published 14 November 2019

Introduction

Plate tectonics is a global process in which partially hydrated and dense oceanic lithosphere is recycled in long lived subduction zones. Although prevalent throughout the Phanerozoic, it is unclear whether, or to what extent, this process operated during the Archean (4.0-2.5 Ga) when mantle heat flow was higher, and the lithosphere was perhaps less differentiated (Brown, 2014; Kamber, 2015). Critical to this debate is the interpretation of tonalite-trondhjemite-granodiorite (TTG) complexes, which make up 90% of the preserved Archean juvenile continental crust (Martin *et al.*, 2005; Moyen and Martin, 2012). These low-K, high-Gd_N/Yb_N, I-type granitoids reflect melting of hydrous basaltic sources with residual hornblende and/or garnet (*e.g.*, Arth and Hanson, 1975; Rapp *et al.*, 1991). Interpretations regarding the geodynamic setting of TTG formation are diverse and numerous (Moyen and Martin, 2012). Several of these consider TTGs as slab melts from primitive flat slab subduction zones with a high geothermal gradient and no contribution from the mantle wedge (Smithies, 2000; Laurent *et al.*, 2014). Others models suggest that TTGs represent melts from thickened mafic crust produced during episodes of density-driven crustal overturning, delamination, underplating or plume activity (Smithies, 2000; Bédard, 2006; van Kranendonk *et al.*, 2007; Kamber, 2015; Johnson *et al.*, 2017). Stagnant lid models (*e.g.*, Debaille *et al.*, 2013) provide hybrids to these 'subduction' and 'intraplate' models (Moyen and Martin, 2012), involving plume-induced melting, as well as flux melting of the mantle during sporadic, local plate burial. Although the models differ at various levels of detail, they differ fundamentally regarding the nature of the mafic source: either it comprised deeply subducted crustal material from the Earth's surface, or it represented the lower and never-before-surfaced sections of a thickened or underplated crust.

Zircon Hf and O isotope data suggest that Archean juvenile continental crust formed by melting of enriched mafic crust extracted from a still primitive mantle, and that sediment recycling and crustal thickening occurred since the Mesoarchean (*e.g.*, Kemp *et al.*, 2010; Næraa *et al.*, 2012; Reimink *et al.*, 2016; Roberts and Santosh, 2018). The same is indicated by Si-O isotope data for Archean detrital zircon (Trail *et al.*, 2018).

1. Department of Earth, Ocean and Atmospheric Sciences, University of British Columbia, 2020-2207 Main Mall, Vancouver V6T 1Z4, Canada
2. Department of Geology, Lund University, Sölvegatan 12, SE- 223 62 Lund, Sweden
3. Department of Earth, Environmental and Biological Sciences, Queensland University of Technology, 2 George Street, Brisbane QLD4000, Australia
4. Institut für Mineralogie, Westfälische Wilhelms-Universität, Corrensstraße 24, D-48149 Münster, Germany
5. Paul Scherrer Institut, Forschungsstrasse 111, CH-5232 Villigen, Switzerland
6. Geological Survey of Canada, 601 Booth Street, Ottawa K1A 0E8, Canada
7. Institut für Geologie, Baltzerstrasse 1+3, CH-3012 Bern, Switzerland
8. Lamont-Doherty Earth Observatory, Columbia University, 61 Route 9W, Palisades, NY 10964, USA
9. Department of Geosciences, 255 Earth and Space Sciences Building, Stony Brook University, Stony Brook, NY 11794-2100, USA
10. Department of Geosciences, Swedish Museum of Natural History, Box 50007, SE-104 05 Stockholm, Sweden
* Corresponding author (email: msmit@eoas.ubc.ca)

These interpretations fit the observation that high $^{18}O/^{16}O$ granitoids produced by melting of surface-altered rocks are restricted to post-Archean time when recycling of such material, possibly by subduction, became prevalent (Valley *et al.*, 2005). Some Archean TTGs show elevated $^{30}Si/^{28}Si$ and $^{18}O/^{16}O$ values, which were interpreted to indicate chert and, by inference, subducted sediments in the source (Deng *et al.*, 2019). The integral Si-O isotope record of Hadean zircon and Archean TTGs indicates source contributions from a variety of supra-crustal rocks, including chemical sediments, serpentinised and silicified basalts (Trail *et al.*, 2018; André *et al.*, 2019). Whether anatexis of such material requires deep burial by subduction is unclear. Moreover, Si and O may not both represent the source and its components. The elevated $^{18}O/^{16}O$ values that — together with elevated $^{30}Si/^{28}Si$ values — were taken to represent the chert component actually partly exceed those typically observed for Archean TTGs; these could reflect secondary ^{18}O-enrichment *via* low temperature alteration (Valley *et al.*, 2005). The Sr anomalies (Sr/Sr*) of the analysed TTGs correlate strongly inversely with $^{18}O/^{16}O$ and may thus likewise be disturbed. Strikingly, the compositions of the samples with highest Sr/Sr* values match those modelled for low degree garnet-stable partial melting of a tholeiitic source that is *not* contaminated by chert or other components (Deng *et al.*, 2019). Although Si-O data provide a unique opportunity to discern supra-crustal contributions to TTG sources (Trail *et al.*, 2018), their interpretation to discern the geodynamic setting of TTG formation is still controversial.

Boron analysis provides an alternative approach to characterising the TTG source. The global B cycle and B isotope systematics are well characterised and appear uniform across geologic time (Supplementary Information, Introduction 1). Most importantly, seawater shows a very strong long term enrichment in the heavy isotope ^{11}B, which is reflected in the B chemistry of subducted slabs and magmatic rocks from active margins (Ryan and Chauvel, 2014; de Hoog and Savov, 2018). The latter is because B is partitioned into melts or fluids that are expelled from the subducting slab and feed the arc source. Due to the enrichment of B and ^{11}B in their source, most magmatic rocks from active margins — including adakites and modern I-type granitoids from continental arcs (Fig. 2) — typically exhibit higher $\delta^{11}B$ values than the average continental crust ($\delta^{11}B$ = -9.4 ± 0.4‰), or mid-oceanic ridge basalts (MORB) and the depleted MORB mantle (DMM; $\delta^{11}B$ = -7.1 ± 0.9‰; Marschall *et al.*, 2017; Marschall, 2018; $\delta^{11}B = 1000 \times [(^{11}B/^{10}B)_{sample}/(^{11}B/^{10}B)_{SRM\text{-}951} - 1]$). Only in rare situations of very steep or very hot subduction do magmatic rocks occasionally include $\delta^{11}B$ values that are similar to, or even lower than, that of DMM. Intense dehydration in these locations cause slab B budgets to be so low that the B signature of the arc source becomes dominated by melting of the mantle wedge (*e.g.*, de Hoog and Savov, 2018).

The B Signature of Archean TTGs

Boron concentrations and isotope compositions were determined for: 1) 3.78 Ga tonalite gneisses from the Isua Greenstone Belt, West Greenland; 2) ≥3.6 Ga tonalite and trondhjemite gneisses from the Acasta Gneiss; 3) 3.58 Ga tonalite gneisses from the Bastar Craton, India; 4) 2.87-2.79 Ga tonalite and trondhjemite gneisses from the Tartôq Greenstone Belt in Southwest Greenland. Whole rock materials were analysed, except for the Acasta TTG samples, which are poly-metamorphosed and exhibit altered matrices. To investigate the initial B composition of these rocks, *in situ* B analysis was done on pristine biotite inclusions inside igneous zircon (rationale in Supplementary Information, Introduction 2; geological descriptions in Supplementary Information, Introduction 3).

The samples show a range of trace element compositions (Table S-7) and comprise low and high Gd_N/Yb_N TTGs (Acasta, Tartôq), or high Gd_N/Yb_N TTGs only (Isua, Bastar; Fig. 1). Boron concentrations are 1.2-3.4 ppm — similar to those observed in other pristine Archean TTGs (Supplementary Information, Introduction 1). The B concentration correlates with Zr/Hf (R^2 = 0.82; Fig. 2a), but not with B/Nb, B/La, B/Zr, Gd_N/Yb_N or Nb/Ta. The $\delta^{11}B$ values of bulk TTG are -15.2 to -2.5‰ (Fig. 3, Table S-5). The $\delta^{11}B$ values correlate negatively with B concentration (R^2 = 0.73; Fig. 2a) and Zr/Hf (R^2 = 0.75; Fig. 2b). The meta-tonalite sample 508281 shows a similar B concentration as pristine samples, yet yielded $\delta^{11}B$ values that are at least 5‰ higher. The $\delta^{11}B$ values of biotite inclusions in Acasta zircon are -5.4‰ or lower, indicating negative $\delta^{11}B$ values for the protolith, even when assuming the largest biotite-melt fractionation factor (Supplementary

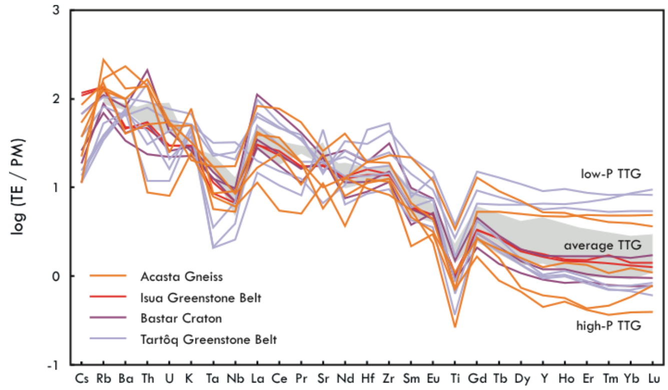

Figure 1 Trace element concentrations for the TTG samples and average TTG (Moyen and Martin, 2012). All data are normalised to primitive mantle (PM; data in Table S-7).

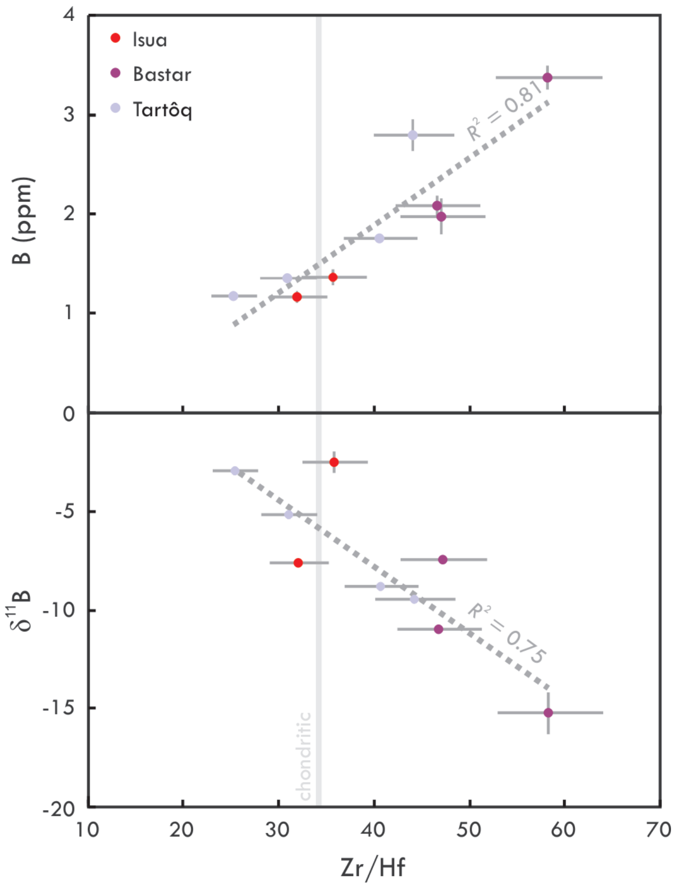

Figure 2 **(a)** B and **(b)** $\delta^{11}B$ versus Zr/Hf with the correlation coefficients for the given regressions.

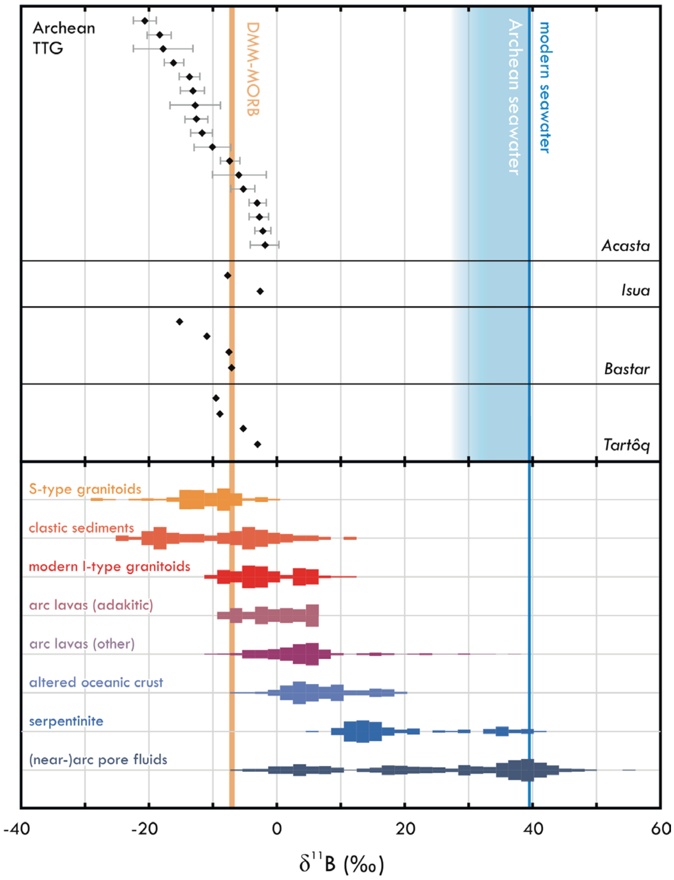

Figure 3 Boron isotope data for the analysed samples and terrestrial reservoirs (histograms). Error bars for whole rock analyses are smaller than the symbols. Acasta data represents bulk rock δ^{11}B modelled from biotite data (Supplementary Information, Analytical Methods and Data). The values for reference reservoirs are in Table S-1.

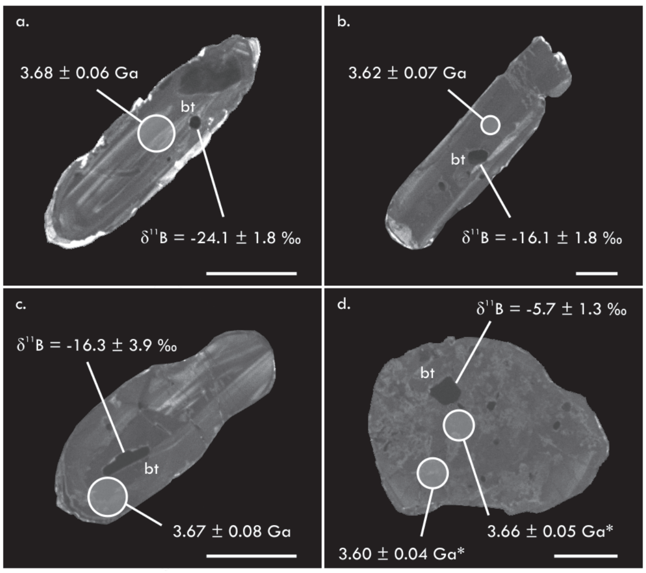

Figure 4 Cathodoluminescence images of zircon from the Acasta Gneiss Complex samples showing analysed biotite inclusions. The δ^{11}B values of biotite (in‰) and the ^{207}Pb/^{206}Pb age of the surrounding zircon (minimum inclusion age) are shown. Analytical spots are to scale; asterisk marks >10% discordance; scale bars are 50 μm. Data are in Table S-9.

Information, Analytical Methods and Data). The lowest values among this range were obtained from pristine zircon domains (Fig. 4a-c), whereas values above -10‰ were obtained for inclusions from zircon with disturbed U-Pb systematics and signs of alteration. The latter inclusions resemble biotite in the altered matrix in terms of B (Fig. 4d, Table S-5). The dispersion in biotite δ^{11}B values for single samples may thus reflect late fluid-rock interaction. The dispersion in biotite δ^{11}B values for single samples may thus reflect late fluid-rock interaction and the high values among the δ^{11}B range may represent ^{11}B enrichment from this process.

Discussion

Changes in the Zr/Hf value of tonalitic melt typically result from the crystallisation of ferromagnesian minerals (Linnen and Keppler, 2002) — biotite + amphibole ± plagioclase in this case, with or without garnet (Supplementary Information, Discussion) — which likewise would enrich the melt in highly incompatible B. The effects of such magmatic differentiation are clearly reflected in the B-Zr/Hf correlation (Fig. 2a). At chondritic Zr/Hf, TTGs are predicted to have 1-2 ppm B and a δ^{11}B value of *ca.* -7‰, which resembles melts from the DMM (1.2-1.3 ppm, -7.1 ± 0.9‰; Marschall *et al.*, 2017). The δ^{11}B-Zr/Hf correlation may be linked to this through the role of H_2O. Crystallisation of basaltic and andesitic magmas is associated with the exsolution of H_2O and other volatiles (Sisson and Layne, 1993). Aqueous fluids in equilibrium with silicate melt preferentially incorporate ^{11}B, such that the more fractionated and hydrous magmas are, the lower δ^{11}B values of the crystallising magmas become (Hervig *et al.*, 2002). The B-Zr/Hf correlation in TTGs from different terranes and with different composition (Fig. 2) shows that their mafic sources — both garnet-present and garnet-absent—had a similar initial B-δ^{11}B-Zr/Hf signature, and evolved without the addition of externally derived B.

The low B concentrations and δ^{11}B values, and their correlation with Zr/Hf, identify Archean TTGs as the differentiated magmatic products of a common mafic source that contained no detectable B from seawater or seawater-altered rocks. The TTGs differ from modern I-type granitoids from active margins; these are variably enriched in B and ^{11}B, independent of the degree of crystal fractionation (de Hoog and Savov, 2018), and do not show fractionation down to the low δ^{11}B values observed here (Fig. 2). As the relevant B reservoirs appear uniform through time (Supplementary Information, Introduction 1), such a signature would be expected for any Archean arc as well — possibly even more so, considering that a contribution from the mantle wedge appears lacking (Martin *et al.*, 2005). A subduction origin for TTGs cannot be *a priori* excluded. However, this would require that slabs were dehydrated such that they lost all B from seawater-altered materials prior to melting. Such dehydration is not seen even in the warmest of modern arcs and appears inconsistent with the hydrous nature of the TTG source (Moyen and Martin, 2012). More importantly, high geothermal gradients during the Archean would favour slab melting over slab dehydration (Martin, 1986; Moyen and Martin, 2012), indicating that B and H_2O would have been expelled from slabs concomitantly, not sequentially. This considered, the data appear more consistent with the TTG formation *via* 'intraplate' processes (Moyen and Martin, 2012) — *e.g.*, crustal thickening, volcanic resurfacing, overturning, delamination, and stagnant lid or 'squishy lid' tectonics (Bédard, 2006; van Kranendonk *et al.*, 2007; Hoffmann *et al.*, 2011; Debaille *et al.*, 2013; Kamber, 2015; Johnson *et al.*, 2017; Rozel *et al.*, 2017) — in which deep hydrated mafic crust with a DMM-like δ^{11}B value melted under the influence of a high or unstable geotherm. The absence of an elevated

$\delta^{11}B$ signature from any supracrustal rocks, which Si-O data indicate were present in the source (André *et al.*, 2019; Deng *et al.*, 2019), could signify B loss from these rocks during residence at depth on timescales that far exceed that of subduction. With subduction processes not clearly reflected in the B data, it would appear that these did not contribute substantially to Archean juvenile crustal growth before 2.8 Ga. If Archean juvenile crustal growth and the start of modern style plate tectonics are at all related, it would appear that the former was the cause, rather than the consequence, of the latter.

Acknowledgements

We thank G.E. Harlow, C. Martin and T. Zack for providing reference materials, and K. Lindén (NRM), L. Kato and V. Lai (UBC) for technical support. The manuscript substantially benefited from constructive reviews by R. Halama and one anonymous reviewer, and by C.J. Hawkesworth, M. Brown, B. Kamber, and H.R. Marschall on a previous version. We thank M. Boyet for editorial handling. This is contribution #619 of the NordSIMS facility, a Swedish-Icelandic research infrastructure. The research was supported by NSERC (Discovery Grant RGPIN-2015-04080 to MAS), CFI and BC-KDF (Grant 229814 to MAS), NSF (MRI Grant EAR-0959524 to ETR), and VR (Grant 2014-06375). KM and AM acknowledge support through SNF (Grant 17452).

Additional Information

Supplementary Information accompanies this letter at http://www.geochemicalperspectivesletters.org/article1930.

Cite this letter as: Smit, M.A., Scherstén, A., Næraa, T., Emo, R.B., Scherer, E.E., Sprung, P., Bleeker, W., Mezger, K., Maltese, A., Cai, Y., Rasbury, E.T., Whitehouse, M.J. (2019) Formation of Archean continental crust constrained by boron isotopes. *Geochem. Persp. Let.* 12, 23-26.

References

André, L., Abraham, K., Hofmann, A., Monin, L., Kleinhanns, I.C., Foley, S. (2019) Early continental crust generated by reworking of basalts variably silicified by seawater. *Nature Geoscience* 12, 769-773.

Arth, J.G., Hanson, G.N. (1975) Geochemistry and origin of the early Precambrian crust of northeastern Minnesota. *Geochimica et Cosmochimica Acta* 39, 325-362.

Bédard, J.H. (2006) A catalytic delamination-driven model for coupled genesis of Archaean crust and sub-continental lithospheric mantle. *Geochimica et Cosmochimica Acta* 70, 1188-1214.

Brown, M. (2014) The contribution of metamorphic petrology to understanding lithosphere evolution and geodynamics. *Geoscience Frontiers* 5, 553-569.

Debaille, V., O`Neill, C., Brandon, A.D., Naenecour, P., Yin, Q.-Z., Matielli, N., Treiman, A.H. (2013) Stagnant-lid tectonics in early Earth revealed by ^{142}Nd variations in late Archean rocks. *Earth and Planetary Science Letters* 373, 83-92.

de Hoog, J.C.M., Savov, I.P. (2018) Boron isotopes as a tracer of subduction zone processes. In: Marschall, H.R., Foster, G.L. (Eds.) *Boron Isotopes – The Fifth Element, Advances in Isotope Geochemistry 6*. Springer, Heidelberg, 217-247.

Deng, Z., Chaussidon, M., Guitreau, M., Puchtel, I.S., Dauphas, N., Moynier, F. (2019) An oceanic subduction origin for Archaean granitoids revealed by silicon isotopes. *Nature Geoscience* 12, 774-778.

Hervig, R.L., Moore, G.M., Williams, L.B., Peacock, S.M., Holloway, J.R., Roggensack, K., (2002) Isotopic and elemental partitioning of boron between hydrous fluid and silicate melt. *American Mineralogist* 87, 769-774.

Hoffmann, J.E., Münker, C., Næraa, T., Rosing, M.T., Herwartz, D., Garbe-Schönberg, D., Svahnberg, S. (2011) Mechanisms of Archean crust formation inferred from high-precision HFSE systematics in TTGs. *Geochimica et Cosmochimica Acta* 75, 4157-4178.

Johnson, T.E., Brown, M., Gardiner, N.J., Kirkland, C.L., Smithies, R.H. (2017) Earth's first stable continents did not form by subduction. *Nature* 543, 239-242.

Kamber, B.S. (2015) The evolving nature of terrestrial crust from the Hadean, through the Archaean, into the Proterozoic. *Precambrian Research* 258, 48-82.

Kemp, A.I.S., Wilde, S.A., Hawkesworth, C.J., Coath, C.D., Nemchin, A.A., Pidgeon, R.T., Vervoort, J.D., DuFrane, S.A. (2010) Hadean crustal evolution revisited: New constraints from Pb–Hf isotope systematics of the Jack Hills zircons. *Earth and Planetary Science Letters* 296, 45-56.

Laurent, O., Martin, H., Moyen, J.-F., Doucelance, R. (2014) The diversity and evolution of late-Archean granitoids: Evidence for the onset of "modern-style" plate tectonics between 3.0 and 2.5 Ga. *Lithos* 205, 208-235.

Linnen, R.L., Keppler, H. (2002) Melt composition control of Zr/Hf fractionation in magmatic processes. *Geochimica et Cosmochimica Acta* 66, 3293-3301.

Marschall, H.R., Wanless, V.D., Shimizu, N., Pogge von Strandmann, P.A.E., Elliott, T., Monteleone, B.D. (2017) The boron and lithium isotopic composition of mid-ocean ridge basalts and the mantle. *Geochimica et Cosmochimica Acta* 207, 102–138.

Marschall, H.R. (2018) Boron isotopes in the ocean floor realm and the mantle. In: Marschall, H.R., Foster, G.L. (Eds.) *Boron Isotopes – The Fifth Element, Advances in Isotope Geochemistry 6*. Springer, Heidelberg, 189-215.

Martin, H. (1986) Effect of steeper Archean geothermal gradient on geochemistry of subduction zone magmas. *Geology* 14, 753–756,

Martin, H., Smithies, R.H., Rapp, R.P., Moyen, J.-F., Champion, D. (2005) An overview of adakite, tonalite trondhjemite granodiorite (TTG), and sanukitoid: relationships and some implications for crustal evolution. *Lithos* 79, 1-24.

Moyen, J.-F., Martin, H. (2012) Forty years of TTG research. *Lithos* 148, 312-336.

Næraa, T., Scherstén, A., Rosing, M.T., Kemp, A.I.S., Hoffmann, J.E., Kokfelt, T.F., Whitehouse, M.J. (2012) Hafnium isotope evidence for a transition in the dynamics of continental growth 3.2 Gyr ago. *Nature* 485, 627-630.

Rapp, R.P., Watson, E.B., Miller, C. (1991) Partial melting of amphibolite/eclogite and the origin of Archean trondhjemites and tonalities. *Precambrian Research* 51, 1-25.

Reimink, J.R., Davies, J.H.F.L., Chacko, T., Stern, R.A., Heaman, L.M., Sarkar, C., Schaltegger, U., Creaser, R.A., Pearson, D.G. (2016) No evidence for Hadean continental crust within Earth's oldest evolved rock unit. *Nature Geoscience* 9, 777-780.

Roberts, N.M.W., Santosh, M. (2018) Capturing the Mesoarchean emergence of continental Crust in the Coorg Block, Southern India. *Geophysical Research Letters* 45, 7444-7453.

Rozel, A.B., Golabek, G.J., Jain, C., Tackley, P.J., Gerya, T. (2017) Continental crust formation on early Earth controlled by intrusive magmatism. *Nature* 545, 332-335.

Ryan, J.G., Chauvel, C. (2014) The subduction-zone filter and the impact of recycled materials on the evolution of the mantle. In: Holland, H.D., Turekian, K.K. (Eds.) *Treatise on Geochemistry 3: The Mantle and Core.* Elsevier, Amsterdam, 479-508.

Sisson, T.W., Layne, G.D. (1993) H_2O in basalt and basaltic andesite glass inclusions from four subduction-related volcanoes. *Earth and Planetary Science Letters* 117, 619-635.

Smithies, R.H. (2000) The Archaean tonalite–trondhjemite–granodiorite (TTG) series is not an analogue of Cenozoic adakite. *Earth and Planetary Science Letters* 182, 115-125.

Trail, D., Boehnke, P., Savage, P., Liu, M.-C., Miller, M.L., Bindeman, I. (2018) Origin and significance of Si and O isotope heterogeneities in Phanerozoic, Archean, and Hadean zircon. *Proceedings of the National Academy of Sciences* 115, 10287-10292.

Valley, J.W., Lackey, J.S., Cavosie, A.J., Clechenko, C.C., Spicuzza, M.J., Basei, M.A.S., Bindeman, I.N., Ferreira, V.P., Sial, A.N., King, E.M., Peck, W.H., Sinha, A.K., Wei, C.S. (2005) 4.4 billion years of crustal maturation: oxygen isotope ratios of magmatic zircon. *Contributions to Mineralogy and Petrology* 150, 561-580.

van Kranendonk, M.J., Smithies, R.H., Hickman, A.H., Champion, D.C. (2007) Secular tectonic evolution of Archean continental crust: interplay between horizontal and vertical processes in the formation of the Pilbara Craton, Australia. *Terra Nova* 19, 1-38.